

Axisymmetric Models

Next we consider **axisymmetric** systems. If we only consider systems for which most orbits are regular, then the **strong Jeans Theorem** states that, in the most general case, $f = f(E, L_z, I_3)$.

From the symmetries of the individual orbits, it is evident that in this case

$$\langle v_R \rangle = \langle v_z \rangle = 0 \quad \langle v_R v_\phi \rangle = \langle v_z v_\phi \rangle = 0$$

Note that, in this case, $\langle v_R v_z \rangle \neq 0$, which is immediately evident when considering a **thin tube orbit**. In other words, in general the **velocity ellipsoid** is not aligned with (R, ϕ, z) .

Thus, in a three-integral model with $f = f(E, L_z, I_3)$ the **stress tensor** contains four unknowns: $\langle v_R^2 \rangle$, $\langle v_\phi^2 \rangle$, $\langle v_z^2 \rangle$, and $\langle v_R v_z \rangle$.

In this case there are two non-trivial Jeans Equations:

$$\begin{aligned} \frac{\partial(\rho \langle v_R^2 \rangle)}{\partial R} + \frac{\partial(\rho \langle v_R v_z \rangle)}{\partial z} + \rho \left[\frac{\langle v_R^2 \rangle - \langle v_\phi^2 \rangle}{R} + \frac{\partial \Phi}{\partial R} \right] &= 0 \\ \frac{\partial(\rho \langle v_R v_z \rangle)}{\partial R} + \frac{\partial(\rho \langle v_z^2 \rangle)}{\partial z} + \rho \left[\frac{\langle v_R v_z \rangle}{R} + \frac{\partial \Phi}{\partial z} \right] &= 0 \end{aligned}$$

which clearly doesn't suffice to solve for the four unknowns.

$f(E, L_z)$ Models I

To make progress, one therefore often makes the additional assumption that the DF has the **two-integral form** $f = f(E, L_z)$.

In this case we have that $\rho = \int_{v^2 < 2\Psi} f(\Psi - \frac{1}{2}v^2, Rv_\phi) d^3\vec{v}$

where we have imposed the usual condition $f = 0$ for $\mathcal{E} < 0$.

Let \vec{v}_m be the **meridional** component of \vec{v} and define the cylindrical coordinates (v_m, v_ϕ, ψ) in velocity space, with

$$v_R = v_m \cos \psi, \quad v_z = v_m \sin \psi$$

then

$$\rho = \int_0^{2\pi} d\psi \int_0^{\sqrt{2\Psi}} v_m dv_m \int_{v_\phi^2 < (2\Psi - v_m^2)} f[\Psi - \frac{1}{2}(v_m^2 + v_\phi^2), Rv_\phi] dv_\phi$$

Note that one can see now that

$$\langle v_R v_z \rangle = \frac{1}{\rho} \int_{v^2 < 2\Psi} v_R v_z f(\Psi - \frac{1}{2}v^2, Rv_\phi) d^3\vec{v} = 0$$

which follows from the fact that $\int_0^{2\pi} \sin \psi \cos \psi d\psi = 0$. Thus, models with $f = f(E, L_z)$ have their **velocity ellipsoid** aligned with (R, ϕ, z) .

$f(E, L_z)$ Models II

In addition, since $\int_0^{2\pi} \sin^2 \psi d\psi = \int_0^{2\pi} \cos^2 \psi d\psi = \pi$ we have that

$$\langle v_R^2 \rangle = \langle v_z^2 \rangle = \pi \int_0^{\sqrt{2\Psi}} v_m^3 dv_m \int_{v_\phi^2 < (2\Psi - v_m^2)} f[\Psi - \frac{1}{2}(v_m^2 + v_\phi^2), Rv_\phi] dv_\phi$$

Thus, we have that

$$f = f(E, L_z) \implies \langle v_R^2 \rangle = \langle v_z^2 \rangle \text{ and } \langle v_R v_z \rangle = 0$$

Now we have two unknowns left, $\langle v_R^2 \rangle$ and $\langle v_\phi^2 \rangle$, and the Jeans equations reduce to

$$\begin{aligned} \frac{\partial(\rho \langle v_R^2 \rangle)}{\partial R} + \rho \left[\frac{\langle v_R^2 \rangle - \langle v_\phi^2 \rangle}{R} + \frac{\partial \Phi}{\partial R} \right] &= 0 \\ \frac{\partial(\rho \langle v_z^2 \rangle)}{\partial z} + \rho \frac{\partial \Phi}{\partial z} &= 0 \end{aligned}$$

which can be solved. Note, however, that the Jeans equations provide no information regarding how $\langle v_\phi^2 \rangle$ splits in streaming and random motions.

In practice one often follows Satoh (1980), and writes that

$\langle v_\phi \rangle^2 = k \left[\langle v_\phi^2 \rangle - \langle v_R^2 \rangle \right]$. Here k is a free parameter, and the model is **isotropic** for $k = 1$.

$f(E, L_z)$ Models III

Now let us return to our expression for the density ρ . If we change the variables of integration from (v_m, v_ϕ) to (\mathcal{E}, Ψ) , we obtain

$$\begin{aligned}\rho &= \frac{2\pi}{R} \int_0^\Psi d\mathcal{E} \int_{L_z^2 < 2(\Psi - \mathcal{E})R^2} f(\mathcal{E}, L_z) dL_z \\ &= \frac{2\pi}{R} \int_0^\Psi d\mathcal{E} \int_0^{R\sqrt{2(\Psi - \mathcal{E})}} [f(\mathcal{E}, L_z) + f(\mathcal{E}, -L_z)] dL_z \\ &= \frac{4\pi}{R} \int_0^\Psi d\mathcal{E} \int_0^{R\sqrt{2(\Psi - \mathcal{E})}} f_+(\mathcal{E}, L_z) dL_z\end{aligned}$$

where we have defined f_+ as the part of the DF that is **even** in L_z , i.e.,

$$\begin{aligned}f(\mathcal{E}, L_z) &= f_+(\mathcal{E}, L_z) + f_-(\mathcal{E}, L_z) \\ f_\pm(\mathcal{E}, L_z) &\equiv \frac{1}{2} [f(\mathcal{E}, L_z) \pm f(\mathcal{E}, -L_z)]\end{aligned}$$

We thus see that the density depends only on the even part of the DF (i.e., the density contributed by a star does not depend on its sense of rotation). This also implies that there are infinitely many DFs $f(E, L_z)$ that correspond to exactly the same $\rho(R, z)$, namely all those that only differ in $f_-(\mathcal{E}, L_z)$.

$f(E, L_z)$ Models IV

Thus, given a density distribution $\rho(R, z)$, one can in principle obtain a unique $f_+(\mathcal{E}, L_z)$. In practice, the computation of $f_+(\mathcal{E}, L_z)$ was considered very difficult.

It was thought that one needs to (i) be able to express ρ explicitly as a function of R and Ψ , and (ii) perform a complicated integral transform.

However, this situation changed drastically when Hunter & Qian (1993) derived an axisymmetric analogue of **Eddington's Formula** based on a **complex contour integral**, which does not require explicit knowledge of $\rho(R, \Psi)$.

In addition, Evans (1993, 1994) has found a large and useful family of models for which all relevant calculations can be done analytically. This is the family of **power-law models**, which we already encountered in the exercises.

So for a wide range of $\rho(R, z)$, we can compute the unique, corresponding $f_+(\mathcal{E}, L_z)$. But what about the odd part of the DF, $f_-(\mathcal{E}, L_z)$?

While $f_-(\mathcal{E}, L_z)$ has no influence on the **density distribution**, it specifies the asymmetry between clockwise and counter-clockwise orbits. Hence, it is responsible for the **mean streaming velocity**.

$f(E, L_z)$ Models V

In fact, it is straightforward to show that

$$\langle v_\phi \rangle = \frac{4\pi}{\rho R^2} \int_0^\Psi d\mathcal{E} \int_0^R \sqrt{2(\Psi - \mathcal{E})} f_-(\mathcal{E}, L_z) L_z dL_z$$

In principle, if we were to know $\langle v_\phi \rangle(R, z)$, we could solve for $f_-(\mathcal{E}, L_z)$ using the Hunter & Qian **complex contour integral** method, just like we can recover $\rho(R, z)$ from $f_+(\mathcal{E}, L_z)$.

In practice, the observationally accessible quantities are $\Sigma(x, y)$ and $v_{\text{los}}(x, y)$. Unless the system is seen edge-on, one can not uniquely deproject these for $\rho(R, z)$ and $\langle v_\phi \rangle(R, z)$.

$f(E, L_z)$ Models VI

Most $f(E, L_z)$ -modelling therefore uses the following methodology:

- (1a) Assume functional form for $\nu(R, z)$ and value for inclination angle i .
Project ν along line-of-sight and adjust free parameters by fitting $\Sigma(x, y)$.
- (1b) Assume value for i and **deproject** $\Sigma(x, y)$ using some assumptions. Examples are the Richardson-Lucy algorithm (Binney, Davies & Illingworth 1990) and the Multi-Gaussian-Expansion method (Emsellem, Monnet & Bacon 1994). Warning, unless $i = 90^\circ$ these are not unique!
- (2) Assume mass-to-light ratio, $\Upsilon(R, z)$, and compute $\Psi(R, z)$ from $\rho(R, z) = \Upsilon(R, z)\nu(R, z)$ using the **Poisson equation**.
- (3) Solve **Jeans Equations** for $\langle v_R^2 \rangle(R, z)$ and $\langle v_\phi^2 \rangle(R, z)$.
- (4) Make assumptions regarding split of $\langle v_\phi^2 \rangle$ in streaming motion and random motion (i.e., pick a value for the Satoh k -parameter).
- (5) Project model and compare resulting $v_{\text{los}}(x, y)$ and $\sigma_{\text{los}}(x, y)$ to data obtained from spectroscopy.
- (6) Repeat analysis to constrain i, k and $\Upsilon(R, z)$.

For examples, see Binney, Davies & Illingworth (1990), van der Marel (1991), Cretton & van den Bosch (1999)

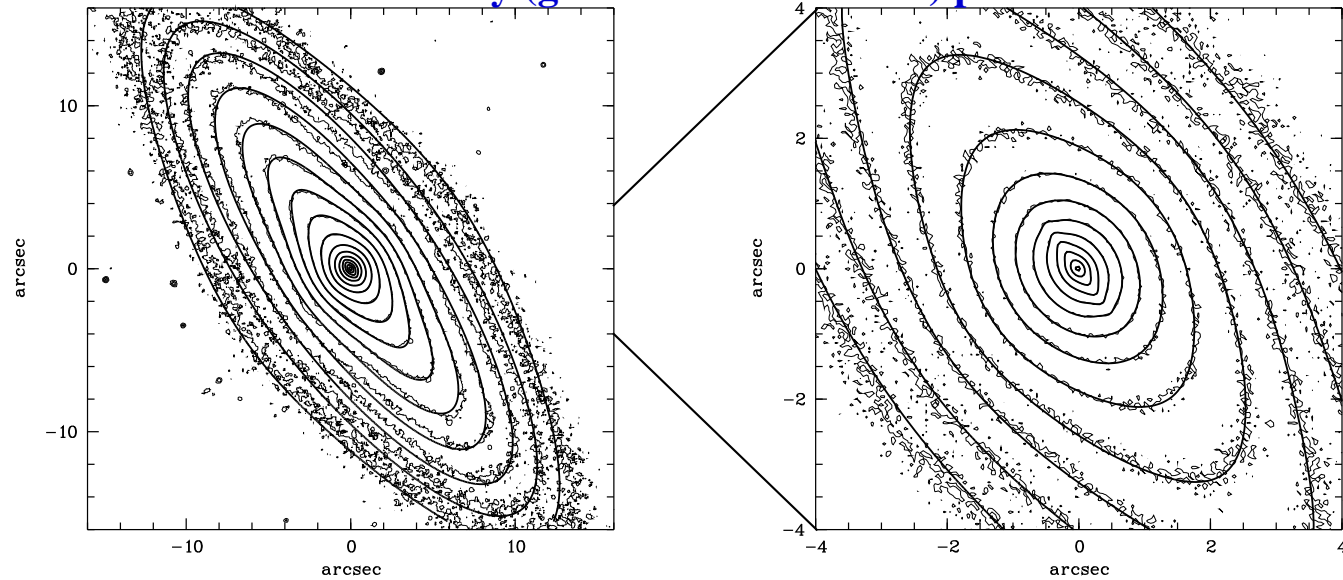
$f(E, L_z)$ Models VII

The results of $f(E, L_z)$ modeling can be summarized as follows

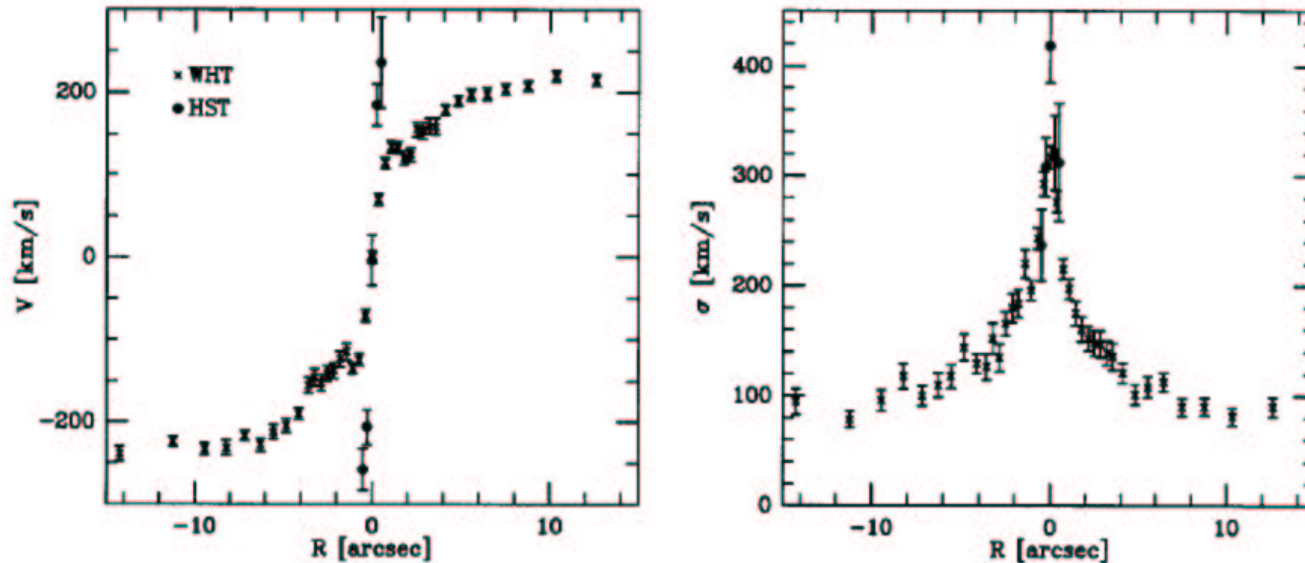
- Because $\sigma_R = \sigma_z$, flattening of **oblate** models must come from large ϕ -motions; f must be biased towards high- L_z orbits.
- Prolate models require a **deficit** of high L_z orbits. Strongly elongated, prolate systems with $f = f(E, L_z) > 0$ do not exist.
- Isotropic oblate models, i.e. those with $k = 1$, in general give poor fits to the data.
- Anisotropic models fit some galaxies, but not all; those must have $f(E, L_z, I_3)$ or be triaxial.
- There is a **degeneracy** between the mass-to-light ratio and the anisotropy (e.g., Binney & Mamon 1982). Can be broken by using **higher-order Jeans Equations** plus observational constraints on **LOSVD shape** (e.g., skewness & kurtosis).
- Several studies have used these models to argue in favor of massive black holes. However, if $f(E, L_z)$ model can only fit data with BH, this is still no proof: need to show that $f \geq 0$, and that no $f(E, L_z, I_3)$ models **without** BH can fit data equally well.

Example: NGC 4342

Photometry (ground-based + HST) plus MGE fit.

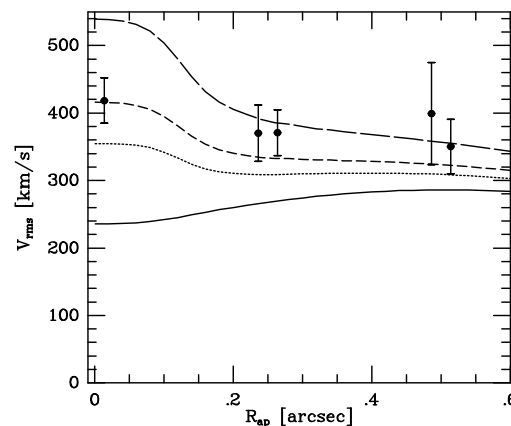
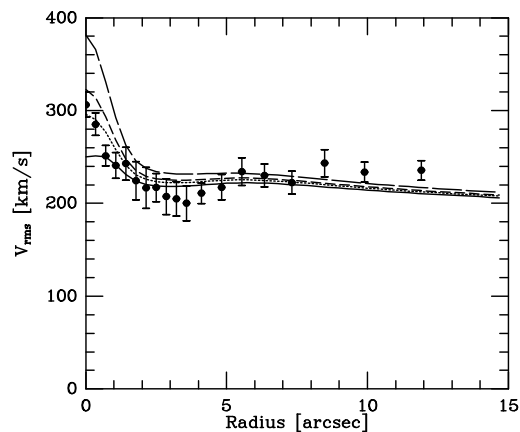
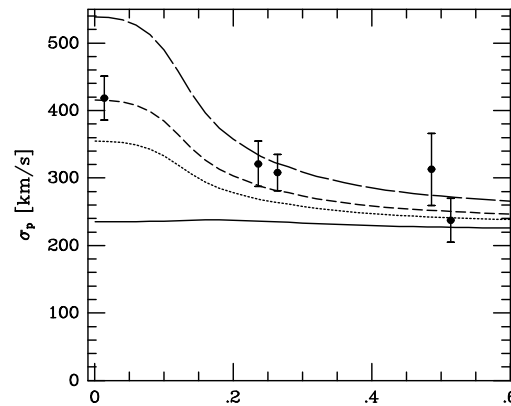
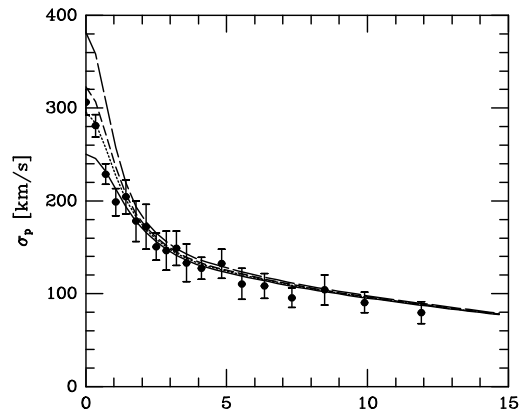
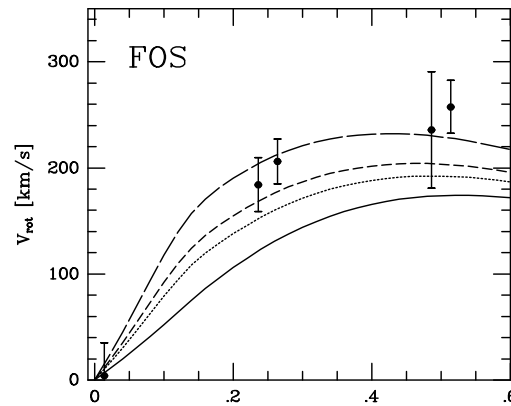
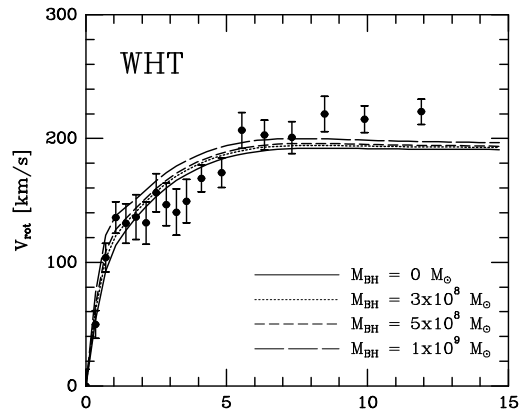


Rotation velocities and velocity dispersions along major axis (WHT + HST)



(from: Cretton & van den Bosch 1999)

Example: NGC 4342



Jeans Models

$$k = 1, i = 90^\circ$$

σ_p in center requires BH

Note: v_{rms} is not well fitted

This is independent of the assumed value for k , which

only determines how v_{rms} splits in v_{rot} and σ_p

$$\Rightarrow f = f(E, L_z, I_3)$$

(Cretton & van den Bosch 1999)

Three-Integral Models

In our discussion on orbits we have seen that most orbits in realistic, axisymmetric galaxy potentials are **regular**, **quasi-periodic**, and confined to the surfaces of **invariant tori**.

Therefore, most orbits admit three **isolating integrals of motion** in involution. According to **strong Jeans Theorem**, we thus expect $f = f(E, L_z, I_3)$.

In this case the two non-trivial **Jeans equations** have four unknowns and can not be solved. In addition, there is no equivalent of **Eddington's formula** to obtain “ f from ρ ”.

In the past, **axisymmetric three integral models** have been constructed using

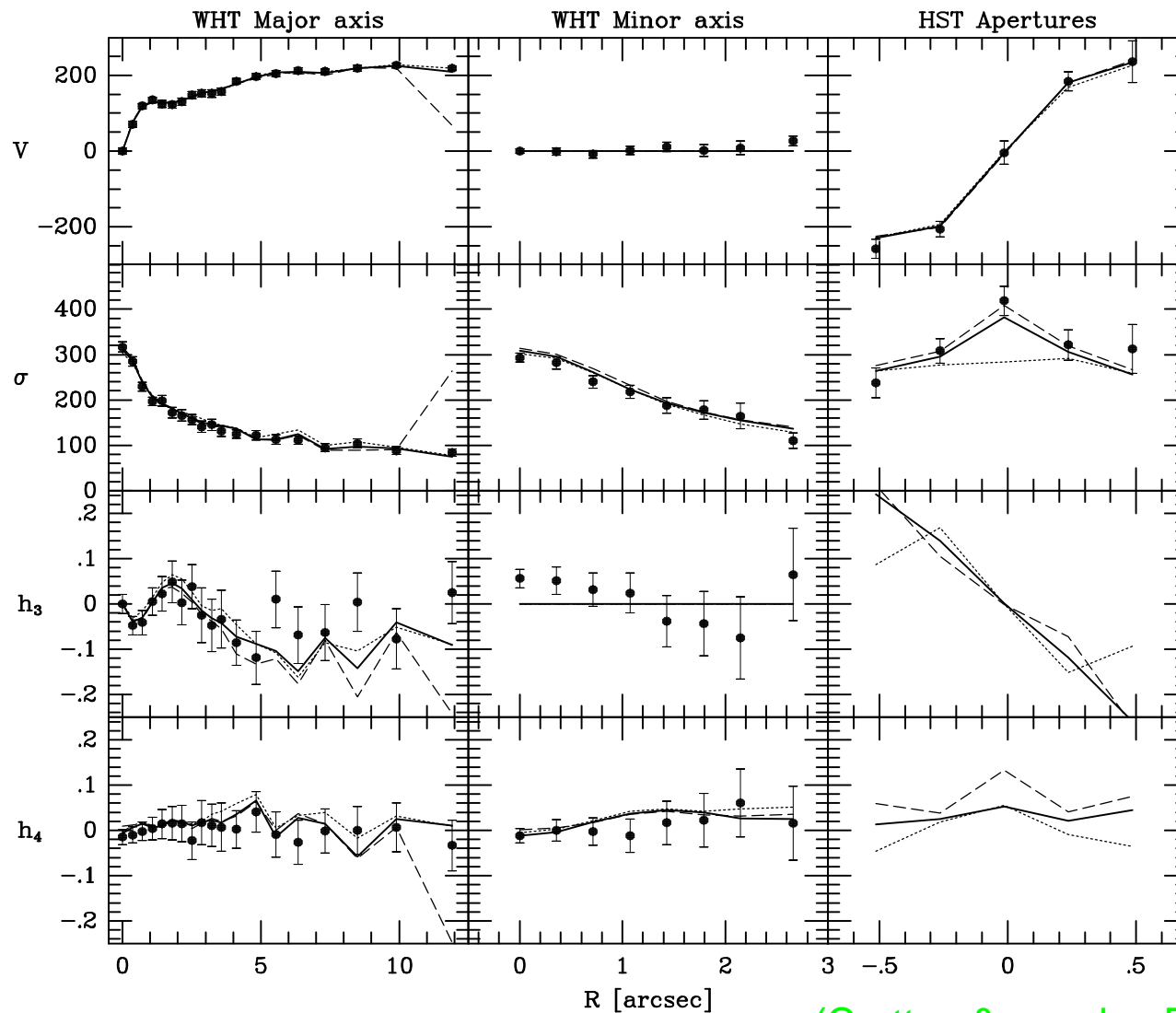
- special, separable potentials (Stäckel potentials), for which I_3 is known exactly (Bishop 1986; de Zeeuw & Hunter 1990)
- approximate third integrals (Petrou 1983). The most detailed work along this direction is due to Dehnen & Gerhard (1993), who evaluated the approximate I_3 from resonant perturbation theory.
- orbit superposition techniques. These are based on integrating large numbers of orbits, and then to find the combination of orbits that best matches the data (Schwarzschild 1979; Richstone 1984; Cretton et al. 1999). This method has recently received much attention.

Three-Integral Models

Schwarzschild's orbit superposition technique for modelling axisymmetric galaxies is based on the following steps:

- (1) Use techniques described above to obtain model for 3D light distribution $\nu(R, z)$, under an assumed value for the inclination angle i .
- (2) Assume a value for the stellar mass-to-light ratio Υ , and compute the corresponding potential $\Psi(R, z)$ from the **Poisson equation**. To this potential one may add that of a **central BH** and/or a **dark matter halo**.
- (3) Integrate a **large sample** of orbits in the total potential. Make sure to cover full allowed ranges of E , L_z , and I_3 : sampling (E, L_z) -space is trivial, while I_3 is sampled by location of turning point on **zero-velocity curve**.
- (4) Compute for each orbit k its contribution a_{kj} to each observable j , such as the value of the **velocity profile** $\mathcal{L}(v_j)$ at the projected location (x_j, y_j) .
- (5) Find the orbital weights $w_k \geq 0$ that minimize the quantity $\sum_j [\mathcal{L}(x_j, y_j, v_j) - \sum_k w_k a_{kj}]^2$. Since the number of orbits is typically much larger than the number of observational constraints, this is typically done using a **Non-Negative Least Squares** algorithm.
- (6) Repeat entire analysis for different i , Υ , M_{BH} , etc. in order to constrain these free parameters.

Example: NGC 4342



(Cretton & van den Bosch 1999)

Models without BH are now clearly ruled out. Note though, that unlike the 2I Jeans models, the 3I models can accurately fit the ground-based $V(R)$ and $\sigma(R)$. This owes to the larger amount of freedom of these models.

Triaxial Systems I

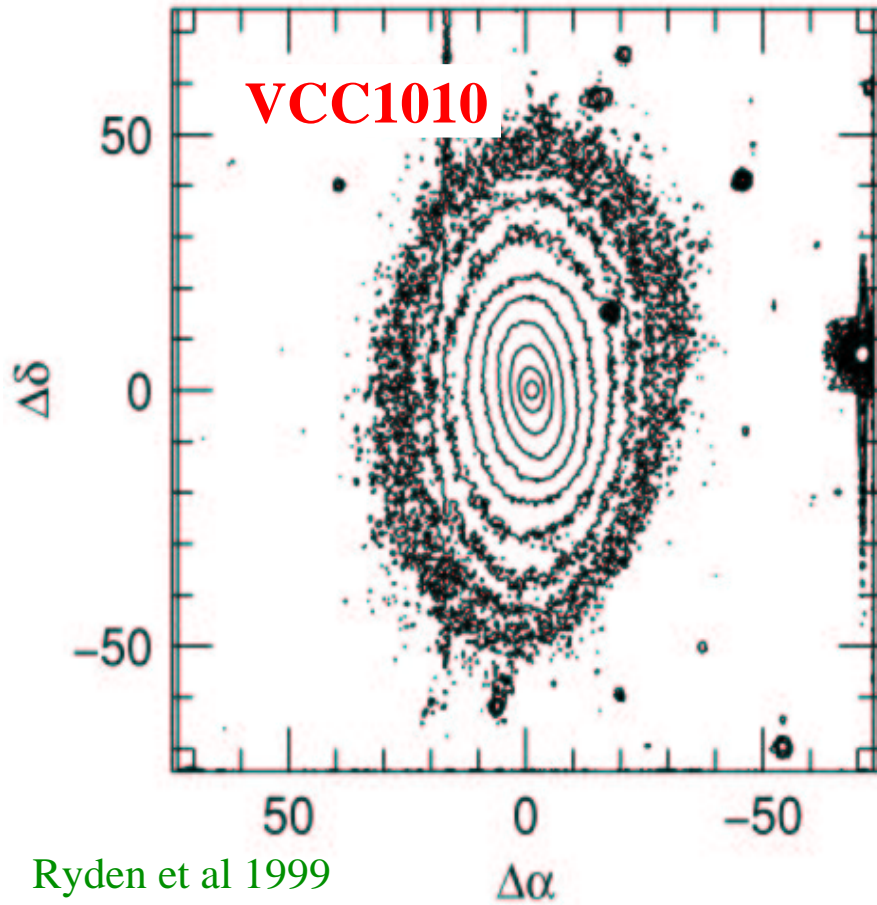
The dynamics of triaxial systems is much more complicated than that of axisymmetric or spherical systems. The main reasons are the lack of symmetry, and the presence of four main orbit families (as opposed to one).

Motivation for considering Triaxial Systems

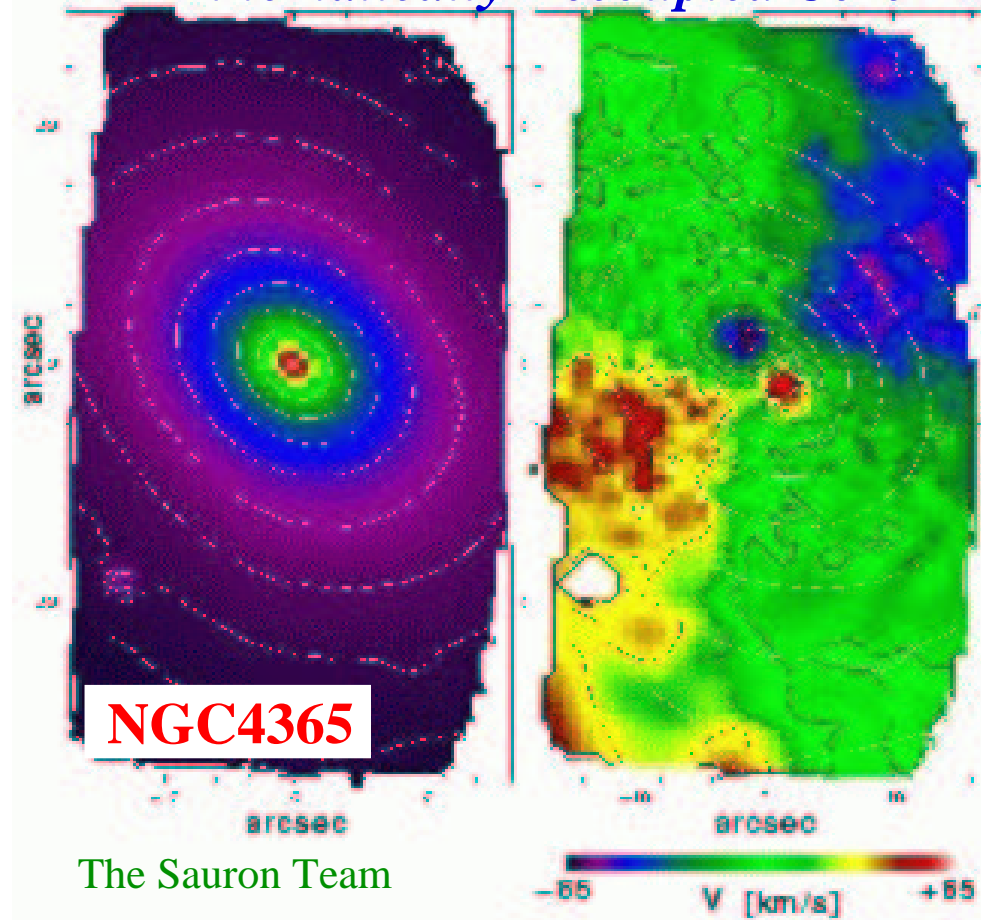
- Slow rotation of (massive) ellipticals (Bertola & Capaccioli 1975; Illingworth 1977) implies that they are inconsistent with **isotropic oblate rotators**. They are supported by **anisotropic pressure**, and, as argued by Binney (1978), are therefore more likely to be triaxial than axisymmetric.
- Some ellipticals reveal zero-velocity curves that are **misaligned** with principal axes. This implies triaxiality, as the presence of both long- and short-axis tubes means that the total angular momentum vector may point anywhere in the plane containing both the long and the short axes (Franx, Illingworth & de Zeeuw 1991).
- Some galaxies reveal **isophotal twists**, in which the position angle of the isophotes changes with radius. This has a most natural explanation if these systems are triaxial with axis ratios that vary with radius (e.g., Stark 1977)
- Numerical simulations show that collapsed haloes are often triaxial (van Albada 1982; Warren et al. 1992)

Observational Hints for Triaxiality

Isophotal Twist



Kinematically Decoupled Core



Triaxial Systems II

But, case for triaxiality may not be that strong:

- N -body simulations that include a **dissipative component** often reveal evolution towards axisymmetry (Udry 1993; Dubinsky 1994)
- Presence of **central BH** tends to drive system towards axisymmetry (Norman, May & van Albada 1985; Merritt & Quinlan 1998). In both cases, this is due to fact that box orbits become stochastic in steep potential.
- In realistic systems with steep central cusp large fraction of phase-space is occupied by **stochastic orbits**. Precludes stationary triaxial solutions (Schwarzschild 1993; Merritt 1997).
- Anisotropic pressure in axisymmetric systems can also explain slow-rotators if system has sufficient amount of **counter-rotation**. Some axisymmetric systems like this are known (e.g., NGC 4550; Rix et al. 1992).
- Low luminosity ellipticals, in general, lack isophotal twists, are strongly cusped, and are rotationally supported: they are perfectly consistent with being axisymmetric (Bender et al. 1989; Ferrarese et al. 1994; Faber et al. 1997).

Self-Consistent Triaxial Models

In triaxial systems that are close to separable (i.e., most orbits are regular), the **strong Jeans Theorem** implies that $f = f(E, I_2, I_3)$.

The seminal work of Schwarzschild (1979, 1982) showed that **self-consistent** models of triaxial systems exist, both with stationary figures and with slowly tumbling figures. To this extent he used orbit superposition techniques.

In particular, Schwarzschild's work has shown that many different orbital configurations, i.e., many different $f(E, I_2, I_3)$, can produce the same density distribution. However, these can have very different kinematical structures (Statler 1987, 1991).

The **orbit superposition technique** only works well when most orbits are regular (in separable potentials, or in potentials with large cores).

In more realistic systems with central cusps, large fraction of phase-space is occupied by **stochastic orbits**. These are difficult to deal with in orbit-superposition techniques: depends on rate of stochastic diffusion.

Most work has focussed on class of **separable** (Stäckel) potentials (Kuzmin 1973; de Zeeuw 1985) and on **scale-free** potentials (Gerhard & Binney 1985). Probably these are not very realistic, but they provide useful insight